Broadband Frequency-Hopping Radar With Fourier Domain Mode-Locking Period-One Laser Dynamics

Xiaoyue Yu, Fangzheng Zhang, *Senior Member, IEEE*, Qing Xiong, Xin Yan, Yansen He, *Student Member, IEEE*, Gong Zhang, *Senior Member, IEEE*, Shilong Pan, *Fellow, IEEE*, and Yuan Yu, *Member, IEEE*

***Abstract*—A frequency hopping (FH) radar based on period-one oscillation laser dynamics with Fourier domain mode-locking (FDML) is proposed and experimentally demonstrated. In the transmitter, a broadband FH signal is generated by adjusting injection strength through intensity modulation. By further incorporating an optoelectronic feedback loop with the temporal period of the FH signal matched with its round-trip delay, the frequency stability and accuracy are greatly improved. In the receiver, to reduce the sampling rate and computational complexity, self-referenced frequency down conversion is applied and a kernel function correlation algorithm is adopted in digital signal processing to procure the high-resolution range profile. In the experiment, an FH signal with a bandwidth of 8 GHz is generated, based on which the detections of single-target and two-targets are demonstrated respectively, achieving a range resolution of 2.15 cm. The proposed photonics-based FH radar with FDML-based P1 dynamics for signal generation is supposed to find more applications in further high-resolution radar detection and imaging.**

***Index Terms*—Frequency hopping radar, microwave photonics, Fourier domain mode-locking, optical injection and P1 dynamics.**

I. Introduction

IN THE past few decades, Frequency-Hopping (FH) microwave signals have attracted tremendous attention on account of zero inter-symbol interference and anti-intercept capability [1]. For an FH signal, its carrier frequency changes according to a predetermined law [2], [3]. Traditionally, electrical signal generators encounter challenges in generating broadband FH signals with fast FH speed. In recent years, microwave photonic techniques have been studied by reason of the unique features of photonics, including fast signal processing, flat spectral response, ultrawide bandwidth, and electromagnetic interference immunity [4], [5], [6], [7]. For instance, a microwave FH signal could be generated via switching the bias voltage of a Mach-Zehnder modulator [8]. This method has a compact structure but suffers from limited number of frequency points. In [9], a rectangular optical pulse train is generated by intensity modulation and injected into an optical frequency shifting loop. After optical-to-electrical conversion, an electrical frequency-stepped signal can be obtained. This method has nano-second FH speed and reconfigurable frequency intervals, but it cannot generate arbitrary FH signals. Microwave FH signals can also be generated through either frequency-to-time mapping or space-to-time mapping [10] combined with optical pulse shaping. However, the foremost restriction is that these systems have high complexity and poor frequency agility. To balance the frequency fineness and FH speed, the generation of FH signal based on period-one (P1) oscillation laser dynamics has been proposed and demonstrated [11], [12]. After optical injection, FH signals with fast hopping speed of up to nanosecond level can be generated by flexibly adjusting the optical power of injected light. In [11], wideband stepped-frequency and Costas sequence FH signals are successfully generated. While, the intrinsic noise of semiconductor laser deteriorates the frequency stability, making it challenging to implement high-resolution radar detection and imaging.

In this letter, we propose a photonics-based broadband FH radar system based on P1 dynamics of a semiconductor laser, in which the Fourier Domain Mode-locking (FDML) is applied to improve the quality of the generated FH signals. In the experiment, an FH signal having 8 GHz bandwidth (10-18GHz) is generated. By introducing the optoelectronic feedback loop to realize FDML, the linewidth and frequency stability of generated FH signal are significantly improved. Furthermore, radar ranging experiments of single-target and two-targets are conducted. To decrease the sampling rate and computational complexity, a high-resolution range profile algorithm based on the kernel function correlation method is applied to the self-referenced frequency down-converted echo signal, through which the obtained range resolution reaches 2.15 cm. These results verify the validity of the proposed FH radar system and ranging algorithm.

II. Principle

The schematic configuration of the proposed broadband FH radar system is depicted in Fig. 1. The master laser (ML) produces a continuous wave light, which is sent to a

Received 28 February 2025; revised 22 May 2025; accepted 22 June 2025. Date of publication 24 June 2025; date of current version 3 July 2025. This work was supported in part by the National Natural Science Foundation of China under Grant 62371224, in part by Shanghai Aerospace Science and Technology Innovation Fund under Grant SAST2024-023, in part by the Open Project Program of Wuhan National Laboratory for Optoelectronics under Grant 2022WNLOKF002, in part by the Open Fund of IPOC (BUPT), in part by the Fundamental Research Program for Young Student of National Key Laboratory of Microwave Photonics under Grant 24-JSKY-ZZKT-QNXS-01, and in part by the Postgraduate Research and Practice Innovation Program of Jiangsu Province. *(Corresponding authors: Fangzheng Zhang; Gong Zhang.)*

Xiaoyue Yu, Fangzheng Zhang, Qing Xiong, Xin Yan, Yansen He, Gong Zhang, and Shilong Pan are with the National Key Laboratory of Microwave Photonics, Nanjing University of Aeronautics and Astronautics, Nanjing 210016, China (e-mail: zhangfangzheng@nuaa.edu.cn; gzhang@nuaa.edu.cn).

Yuan Yu is with Wuhan National Laboratory for Optoelectronics, Huazhong University of Science and Technology, Wuhan 430074, China.

Color versions of one or more figures in this letter are available at https://doi.org/10.1109/LPT.2025.3582759.

Digital Object Identifier 10.1109/LPT.2025.3582759

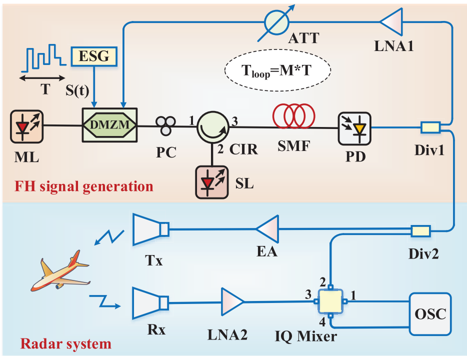

Fig. 1. The schematic configuration of the proposed broadband FH radar system.

dual-drive Mach-Zehnder modulator (DMZM). A low-speed electrical signal generator (ESG) is applied to generate specially designed multi-level electrical control signal, which is launched to one of the radio-frequency (RF) ports of DMZM. After optical intensity modulation at the DMZM, its output power varies with time. Then, the modulated optical signal is injected into the slave laser (SL) via an optical circulator (CIR), in which a polarization controller (PC) used before the CIR is applied to match the polarization state of the ML with that of the free-running SL. By properly adjusting the injection parameters, P1 oscillation is excited in the cavity of the SL, which is manifested as asymmetric single sideband modulation generating a red-shifted optical sideband and a regenerated optical carrier. In this process, the red-shift wavelength is dependent on the change of refractive index inside the cavity, which is subjected to the detuning frequency and injection strength. Here, the detuning frequency is termed as the frequency difference between the ML and the free-running SL. The injection strength is described as the amplitude ratio of the injected light to the free-running SL [12]. For a proper detuning frequency, when a control signal generated by the ESG is loaded to the DMZM to change the injection strength, the red-shift sideband output from the SL will be fast changed with time. After optical-to-electrical conversion by a photodetector (PD), a microwave FH signal is generated, of which the bandwidth and frequency coding can be adjusted by properly setting the control signal and tuning the injection parameters. However, the generated FH signal usually suffers from strong damping oscillation owing to the laser transient properties including the relaxation oscillation, self-pulsation, and turn-on delay [13]. Especially, the amplitude of damping oscillation varies directly with the frequency abrupt range, which deteriorates the frequency stability of the generated FH signal.

To improve the performance of generated FH signals, FDML technique is introduced, which is equivalent to a transient filter used to select different longitudinal modes of a feedback loop. In Fig. 1, the output signal from the SL is transmitted through a span of side mode fiber (SMF) and sent to a PD. Then, an electrical divider (Div1) is used to split a fraction of the FH signal as the optoelectronic feedback signal, which is input to the other RF port of the DMZM to close the feedback loop. A low noise amplifier (LNA1) is utilized to boost the power of the generated FH signal, and a tunable electrical attenuator (ATT) is followed to adjust the optoelectronic feedback strength. When the temporal period T of generated FH signal matches with the round-trip delay of the feedback loop T_{loop} ($T_{loop} = \mathrm{M}\times T$, M is a positive integer), through which the FDML is implemented [14], [15]. In this case, each instantaneous frequency propagating through the feedback loop is phase-locked to the same frequency and can be reinjected locking the SL. Hence, a stable FH microwave signal is generated, of which the instantaneous frequency f is expressed as:

$$f(n,t) = \sum_{n=1}^{N} rect\left(\frac{t - nT_p}{T}\right) \exp(j2\pi f_n t) \quad (1)$$

where $T_p = T/N$ is pulse repetition period, n ($1 \le n \le N$) is the burst index, N is the totally number of frequency points, f_n is frequency of n^{th} burst.

Afterwards, the generated FH signal from the other output port of Div1 is partitioned into two branches by Div2. The FH signal in one branch is injected into the local oscillator (LO) port of an electrical IQ mixer as a reference for radar receiver. The FH signal in the other branch is boosted by an electrical amplifier (EA) and subsequently transmitted by a horn antenna (Tx) for target detection. Meanwhile, another horn antenna (Rx) is utilized to collect the radar echoes, which are amplified by another LNA2 before launched to the RF port of the electrical IQ mixer. Hereto, self-referenced frequency down-conversion of the broadband FH radar echoes is implemented. The output I channel and Q channel signals from the mixer are captured by a real-time oscilloscope (OSC), and digital signal processing is applied to get the target information.

Because of the random FH properties, the range profile cannot be synthesized by fast Fourier transform (FFT) algorithm used in traditional radar receivers. In addition, the sampling frequency down-converted echoes are stochastic. Thus, conventional or Inverse Discrete Fourier Transform (IDFT) also cannot be applied directly. To address this problem, the kernel function correlation method is used to construct the ranging profile [16], [17]. According to the frequency coding of transmitted signal, a series of correlation core K related to the detection distance $r = kdr$ are designed, which is expressed as

$$K(n,k) = \exp\left(-j\frac{4\pi}{c} f_n kdr\right) \quad (2)$$

where $c$denotes the light speed, dr is the correlation step, k($0 \le kdr \le R$) is the correlation index, R is the maximum detection range. Here, dr should be less than the range resolution for the accuracy of ranging. The range profile $y(\mathrm{k})$ can be obtained by correlating the frequency down-converted echo signal with the correlation core:

$$y(k) = \sum_{n=1}^{N} f(n,t) K^{*}(n,k) \quad (3)$$

When the detection distance r determined by the correlation core matches the actual target distance, the correlation results become a coherent summation and will reach the maximal peak in the corresponding distance. Thus, the ranging function is realized.

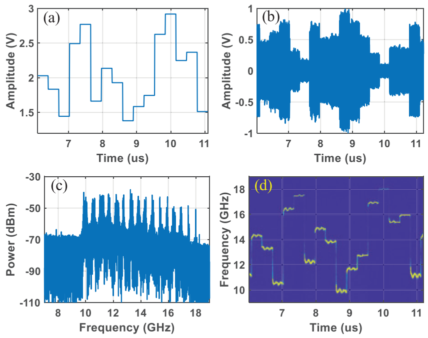

Fig. 2. (a) The specially designed multi-level control signal, (b) the temporal waveform, (c) the electrical spectrum and (d) the time-frequency diagram of the generated FH signal.

III. Experiment and Results

In order to explore the effects of optoelectronic feedback, an FH signal generation system without feedback is firstly conducted. In the experiment, the wavelength and output power of the ML (ID Photonics, CoBrite) is set as 1548.08 nm and 16 dBm, respectively. The SL is a distributed-feedback semiconductor laser (Wave Optics, DFBM-1550-10-SM-ISN), of which the bias current is set as 21 mA. The corresponding free-running output power is 4.33 dBm and the wavelength is 1548.11 nm, respectively. A 16-level electrical control signal generated by the ESG (RIGOL DG4062, 500 MSa/s) is input to one of the RF ports of the DMZM (Fujitsu, FTM7937EZ) for intensity modulation, which is depicted in Fig. 2(a). Its amplitude is randomly changed from 1.38 V to 2.92 V and the temporal period is set as 5 μs. Here, the control signal is designed to generate frequencies having a uniform distribution within the frequency range of the FH signal, which helps to suppress the side lobes when performing matched filtering in the radar receiver [18]. Subsequently, at the output of PD (Discovery, DSC40S), a broadband FH signal is generated and recorded by a real-time oscilloscope (Keysight UXR0104B, 128 GSa/s). The temporal waveform is presented in Fig. 2(b), of which the temporal period is measured as 5 μs. Fig. 2(c) shows the corresponding electrical spectrum. It is notably that the generated FH signal has a bandwidth of 8 GHz (10-18 GHz) with 16 random discrete frequencies. Moreover, the instantaneous time-frequency diagram calculated by short-time Fourier transformation to the temporal waveform is depicted in Fig. 2(d). A 16-level FH signal is generated. However, obvious damping oscillation appears, resulting in frequency jitter and linewidth broadening in the instantaneous time-frequency diagram.

Next, to improve the quality of the generated FH signal, the optoelectronic feedback loop is enabled. In the experiment, the length of SMF is set as 1 km. The feedback power injected to the DMZM is set as -20 dBm by adjusting the tunable electrical ATT (Talent Microwave, TLVA0.1G-40G-40-10, 0.1-40 GHz). To meet the requirement of FDML, the temporal period of control signal is set to 4.61 μs, which is the same as the round-trip delay of the optoelectronic feedback loop. In this instance, stable FDML is achieved. The electrical spectrum of improved FH signal is depicted in Fig. 3(a). The corresponding time-frequency diagram is illustrated in Fig. 3(b). In comparison to the results in Fig. 2, the 3-dB linewidth of each spectral line is obviously narrowed and the damping oscillation is well suppressed. This leads to enhanced signal coherence, which is essential for pulse accumulation in radar applications. To check this property, pulse-to-pulse cross correlation results are calculated. Fig. 4(a) shows the cross-correlation result between the first and the eighth radar pulses generated without FDML. In Fig. 4(a), the full width at half maximum (FWHM) of the cross-correlation peak is measured to be 2.10 cm and there are strong side lodes, which indicates the incoherence between different pulses. Fig. 4(b) shows the cross-correlation result between the first and the eighth pulses generated with FDML. The FWHM of the cross-correlation peak is about 1.95 cm, which is close to the theoretical range resolution (1.875 cm). In addition, the side lobes are suppressed compared with the result in Fig. 4(a). The results validate the advantage of FDML-based FH signal generation method in achieving good radar detection performance.

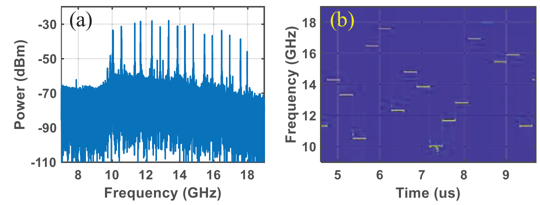

Fig. 3. (a) The electrical spectrum, (b) the time-frequency diagram with the FDML-based optically injected semiconduction laser.

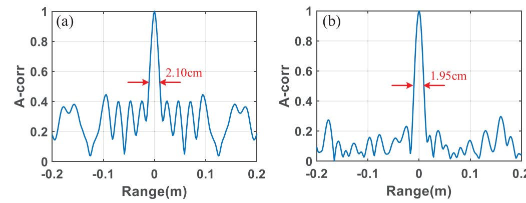

Fig. 4. The pulse-to-pulse cross-correlation results of FH signals generated (a) without FDML and (b) with FDML.

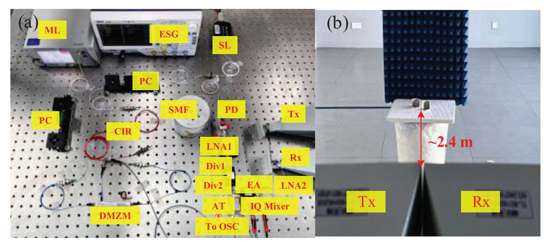

Fig. 5. Photograph of (a) the established broadband FH radar, (b) the detection scenario.

Then, FH radar ranging experiment with the system diagram as depicted in Fig. 5(a) is conducted. In the transmitter, an electrical amplifier (AT microwave, PA-0240-3827X, 2-40 GHz) and a power divider (Talent microwave, RS2W60180-S,6-18GHz) are adopted. Then the transmitting signal is launched to the detection area by a horn antenna (Tx, 8-18GHz). Another reference signal is input into an electrical IQ mixer (Marki MMIQ-0626L, 6-26 GHz). In the receiver, another horn antenna (Rx, 8-18GHz) combined with a low

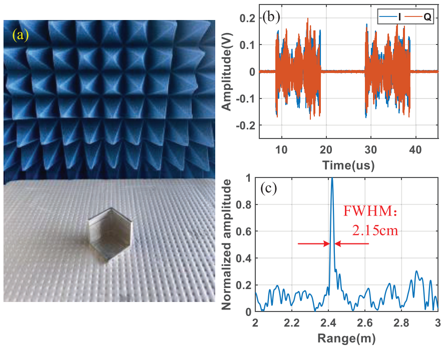

Fig. 6. (a) Single-target detection scenario, (b) the waveforms of I and Q channels from the mixer and (c) the range profile of single-target detection.

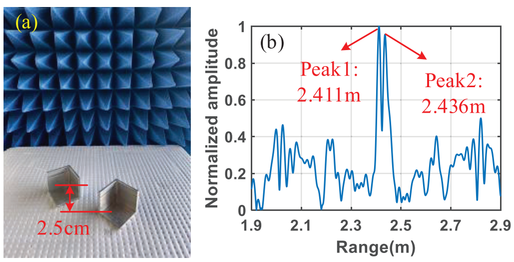

Fig. 7. (a) Two-targets detection scenario, (b) the range profile of two-targets detection.

noise amplifier (AT microwave, LNA-0242-3804C, 2-42 GHz) are used to collect the radar echoes. After frequency mixing in IQ mixer, the output I and Q signals are captured by two channels of the oscilloscope, both with a sampling rate of 500 MSa/s. The target detection scenario is illustrated in Fig. 5(b), in which the targets are places about 2.4 m from the antennas.

First, a trihedral reflector with edge length of 2.3 cm is detected. The detailed detection scenario is depicted in Fig. 6(a). In the experiment, the correlation step dr is set as 0.2 cm. The temporal waveforms from I channel and Q channel of the electrical mixer are depicted in Fig. 6(b). By performing kernel function correlation method, the corresponding range profile is obtained and depicted in Fig. 6(c). A strong peak centered at 2.42 m appears, which corresponding to the distance of real single-target. The FWHM is 2.15 cm and close to the theoretical range resolution.

To further investigate the range resolution, the detection of two targets is conducted, in which two trihedral reflectors are separated by 2.5 cm following the detection path, as illustrated in Fig. 7(a). The obtained range profile is depicted in Fig. 7(b). Two distinguishable peaks matching the two targets emerge at 2.411 and 2.436 m, respectively. The distance between two peaks is measured as 2.5 cm, which agrees well with real values. Again, the results prove the viability of the established FH radar system and algorithm in high-resolution ranging.

IV. Conclusion

In summary, we have proposed a broadband frequency-hopping radar system based on period-one laser dynamics combined with Fourier domain mode-locking and experimentally demonstrated its application in radar ranging. A 16-level FH signal having a bandwidth of 8 GHz (10-18 GHz) is generated. By incorporating a delay-matched optoelectronic feedback loop, the FDML-based technique is enabled, through which the damping oscillation is suppressed and the frequency stability is greatly improved. In addition, by applying a high-resolution range profile algorithm based on the kernel function correlation method, the radar ranging experiments of single-target and two-targets are demonstrated. The sampling rate and computational complexity are significantly reduced. With these advantages, the proposed broadband FH radar system is expected to find more practical applications in further radar systems.

References

[1] C.-Y. Chen and P. P. Vaidyanathan, “MIMO radar ambiguity properties and optimization using frequency-hopping waveforms,” *IEEE Trans. Signal Process.*, vol. 56, no. 12, pp. 5926–5936, Dec. 2008.

[2] M. Strasser, C. Popper, S. Capkun, and M. Cagalj, “Jamming-resistant key establishment using uncoordinated frequency hopping,” in *Proc. IEEE Symp. Security Privacy (SP)*, Oakland, CA, USA, May 2008, pp. 64–78.

[3] Q. Liu and M. P. Fok, “Ultrafast and wideband microwave photonic frequency-hopping systems: A review,” *Appl. Sci.*, vol. 10, no. 2, p. 521, Jan. 2020.

[4] J. Yao, “Microwave photonics,” *J. Lightw. Technol.*, vol. 27, no. 3, pp. 314–335, Feb. 1, 2009.

[5] J. Capmany and D. Novak, “Microwave photonics combines two worlds,” *Nature Photon.*, vol. 1, no. 6, pp. 319–330, Jun. 2007.

[6] F. Zhang, G. Sun, Y. Zhou, B. Gao, and S. Pan, “Towards high-resolution imaging with photonics-based time division multiplexing MIMO radar,” *IEEE J. Sel. Topics Quantum Electron.*, vol. 28, no. 5, pp. 1–10, Sep. 2022.

[7] G. Wu et al., “Bandwidth-enhanced LFM signal generation by period-one dynamics in a directly modulated semiconductor laser,” *Opt. Lett.*, vol. 50, no. 11, p. 3572, Jun. 2025.

[8] Y. Chen, “High-speed and wideband frequency-hopping microwave signal generation via switching the bias point of an optical modulator,” *IEEE Photon. J.*, vol. 10, no. 1, pp. 1–7, Feb. 2018.

[9] Y. Zhang, C. Liu, K. Shao, Z. Li, and S. Pan, “Multioctave and reconfigurable frequency-stepped radar waveform generation based on an optical frequency shifting loop,” *Opt. Lett.*, vol. 45, no. 7, p. 2038, Mar. 2020.

[10] S. T. Cundiff and A. M. Weiner, “Optical arbitrary waveform generation,” *Nature Photon.*, vol. 4, no. 11, pp. 760–766, Oct. 2010.

[11] P. Zhou, F. Zhang, X. Ye, Q. Guo, and S. Pan, “Flexible frequency-hopping microwave generation by dynamic control of optically injected semiconductor laser,” *IEEE Photon. J.*, vol. 8, no. 6, pp. 1–9, Dec. 2016.

[12] x. Yu et al., “Broadband stepped-frequency radar waveform generation by Fourier domain mode-locking period-one laser dynamics,” *Opt. Lett.*, vol. 49, no. 15, p. 4266, Jul. 2024.

[13] G. Arnold and P. Russer, “Modulation behavior of semiconductor injection lasers,” *Appl. Phys.*, vol. 14, no. 3, pp. 255–268, Nov. 1977.

[14] R. Huber, M. Wojtkowski, and J. G. Fujimoto, “Fourier domain mode locking (FDML): A new laser operating regime and applications for optical coherence tomography,” *Opt. Exp.*, vol. 14, no. 8, p. 3225, Apr. 2006.

[15] T. Hao et al., “Breaking the limitation of mode building time in an optoelectronic oscillator,” *Nature Commun.*, vol. 9, no. 1, p. 1839, May 2018.

[16] Z. Liao, D. Lu, J. Hu, and J. Zhang, “Computationally efficient range profile synthesis method based on zero-padding inverse discrete Fourier transform for random stepped frequency radar,” *J. Appl. Remote Sens.*, vol. 13, no. 1, p. 1, Jan. 2019.

[17] Z. Liao, D. Lu, J. Hu, and J. Zhang, “A novel range profile synthesis method for random hopping frequency radar,” in *Proc. IEEE Int. Conf. Digit. Signal Process. (DSP)*, Beijing, China, Oct. 2016, pp. 79–83.

[18] Z. Liao, D. Lu, J. Hu, and J. Zhang, “A low side-lobe waveform design method for random hopping frequency signal,” in *Proc. 9th Int. Conf. Wireless Commun. Signal Process. (WCSP)*, Nanjing, China, Oct. 2017, pp. 1–6.